Supplement of Atmos. Meas. Tech., 8, 523–540, 2015
http://www.atmos-meas-tech.net/8/523/2015/
doi:10.5194/amt-8-523-2015-supplement

Atmospheric Measurement Techniques
Open Access

Supplement of

Pressure-dependent calibration of the OH and HO_2 channels of a FAGE HO_x instrument using the Highly Instrumented Reactor for Atmospheric Chemistry (HIRAC)

F. A. F. Winiberg et al.

Correspondence to: P. W. Seakins (p.w.seakins@leeds.ac.uk)

1 FAGE instrument sensitivity to OH as a function of $[H_2O]_{vap}$

By altering the fractional flow of air through the water bubbler *via* a series of three bypass valves (as shown in Figure 3 in the main text), different H_2O vapour concentrations were passed to the calibrator (200 - 7000 ppmv). Figure S1 shows the instrument sensitivity to OH as a function of $[H_2O]_{vap}$ relative to the C_{OH} measured at 200 ppmv determined using the conventional flow tube calibration method. Calibrations were conducted at a constant laser power ((7 ± 1) mW) and internal cell pressure (3.85 mbar) using the 1.0 mm diameter inlet pinhole and the 200 Hz PRF laser system.

The instrument sensitivity was found to decrease with increasing $[H_2O]_{vap}$ ($\Delta C_{OH} \approx$ -4% (1000 ppmv)$^{-1}$), calculated using the empirical linear regression to the data weighted to the uncertainties in the *x* and *y* axes). The linear regression is purely empirical, and helps to clarify that from the standard operating $[H_2O]_{vap}$ (2000 - 4000 ppmv), any change in C_{OH} falls well within the experimental uncertainty associated with the calibration.

The observed decrease in C_{OH} could be explained by the increased collisional quenching of the OH excited state ($A^2\Sigma^+$ (v'=0)) at higher $[H_2O]_{vap}$, which reduces the OH fluorescence quantum yield, ϕ_{fl}, and the total measurable fluorescence, f_{gate}. As mentioned in the main text (section 5.1.1), the OH fluorescence quantum yield is defined as $\phi_{fl} = A / (A+k_q[M])$, where A is the inverse of the radiative lifetime, and k_q is the rate coefficient for quenching of the excited OH. As $[H_2O]_{vap}$ increases, so does k_q, which in turn decreases ϕ_{fl}, f_{gate} and therfore C_{OH}. Displayed in Figure S1 is the predicted decrease in C_{OH} with increasing $[H_2O]_{vap}$ calculated relative to the C_{OH} at 0 ppmv, which falls well within the calculated uncertainty of the calibration over the experimental range of $[H_2O]$, ~18% to 1σ.

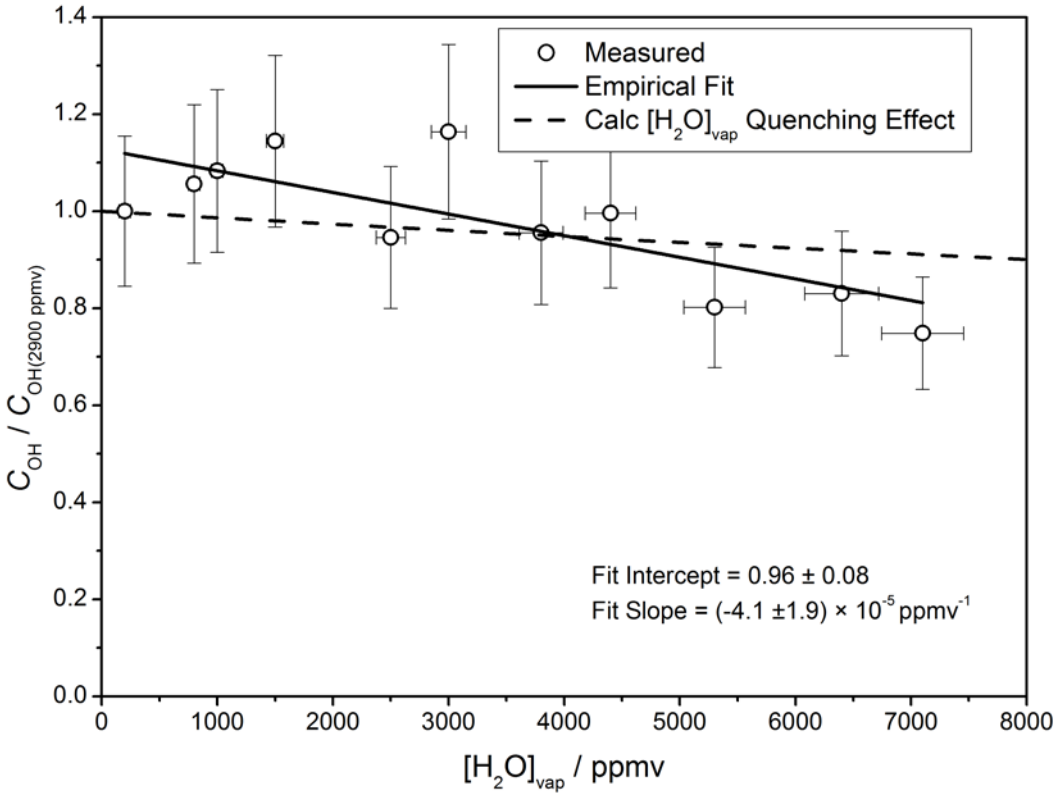

Figure S1. HIRAC FAGE instrument sensitivity to OH, C_{OH}, as a function of $[H_2O]_{vap}$ relative to C_{OH} at 200 ppmv using the LITRON Nd:YAG pumped dye laser system at 200 Hz PRF. All calibrations conducted at constant laser power (7 ± 1 mW) and fluorescence cell pressure (3.84 ± 0.03 mbar) using the 1.0 mm diameter pinhole. Solid line shows the empirical linear regression of the data weighted to the uncertainties in the *x* and *y* axes. Dashed line represents the theoretical effect on the quenching of the OH excited state ($A^2\Sigma^+$ (v'=0)) due to the change in $[H_2O]_{vap}$, displayed relative to the C_{OH} at 0 ppmv. Error bars represent the total uncertainty in the calibration procedure quoted to ±1σ.

2 FAGE instrument sensitivity to OH as a function of laser power

Laser powers entering the OH fluorescence of between 2 and 10 mW were achieved by attenuating the UV light at the dye laser exit aperture using a combination of different neutral density filters (0.2, 0.3 and 0.6 O.D., ThorLabs). The values of C_{OH} for both 200 Hz and 5 kHz PRF laser systems are compared in Figure S2(a) and (b), relative to the C_{OH} at 7 mW (the modal operating laser power). The range of laser powers investigated was designed to encompass the typical operating laser power for the instrument (7 ± 1 mW). All calibrations conducted at constant $[H_2O]_{vap}$ (Figure S2(a) 3300 ± 500 ppmv, (b) 2100 ± 100 ppmv) and internal cell pressure (Figure S2(a) 3.84 ± 0.03 mbar, (b) 3.96 ± 0.04 mbar) with error bars representative of the overall error associated with the calibration process (1σ). Using a linear regression as an empirical measure, a decrease in C_{OH} was observed, with ΔC_{OH} = -20% mW^{-1} at 200 Hz PRF (Figure S2a) and $\Delta C_{OH} \approx$ -3% mW^{-1} at 5 kHz PRF (Figure S2b).

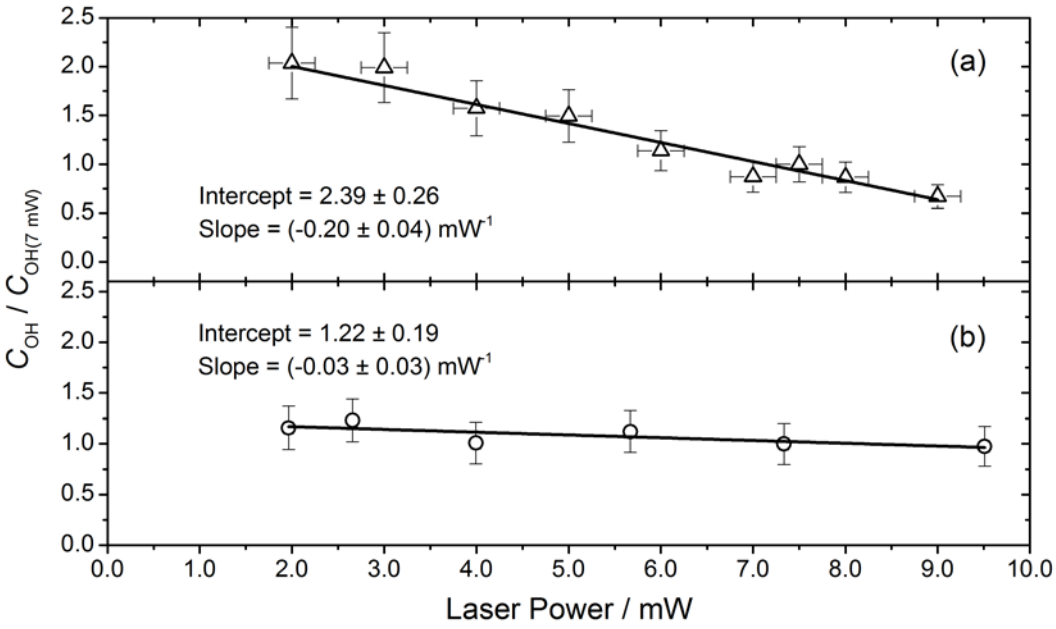

Figure S2. HIRAC FAGE instrumental sensitivity to OH, C_{OH}, relative to C_{OH} at 7 ± 1 mW as a function of laser power entering the OH fluorescence cell for the 200 Hz (a) and 5 kHz (b) Nd:YAG pumped dye laser systems using the H_2O photolysis calibration method. All calibrations conducted at constant $[H_2O]_{vap}$ ((a) 3300 ± 500 ppmv, (b) 2100 ± 100 ppmv) and internal cell pressure ((a) 3.84 ± 0.03 mbar, (b) 3.96 ± 0.04 mbar); uncertainties quoted to ±1σ.

The small decrease in sensitivity to OH as a function of laser power for the 5 kHz PRF laser source was likely due to an increased background S_{OH} measurement from increased laser light

reflections from surfaces inside the cell combined with increased Rayleigh scattering, decreasing the overall S/N ratio. However a more marked decrease was observed in the instrumental sensitivity for the 200 Hz PRF laser system. Upon examination of the $Q_1(2)$ and $Q_{21}(2)$ OH rotational transitions of the OH $A^2\Sigma^+$ (v'=0) ← $X^2\Pi_i$ (v''=0) transition near 308 nm measured OH emission bands measured using the 200 Hz PRF laser at (5.0 ± 0.5) and (24.0 ± 0.5) mW (Figure S3a and b respectively), a broadening of the lines was observed at higher laser powers.

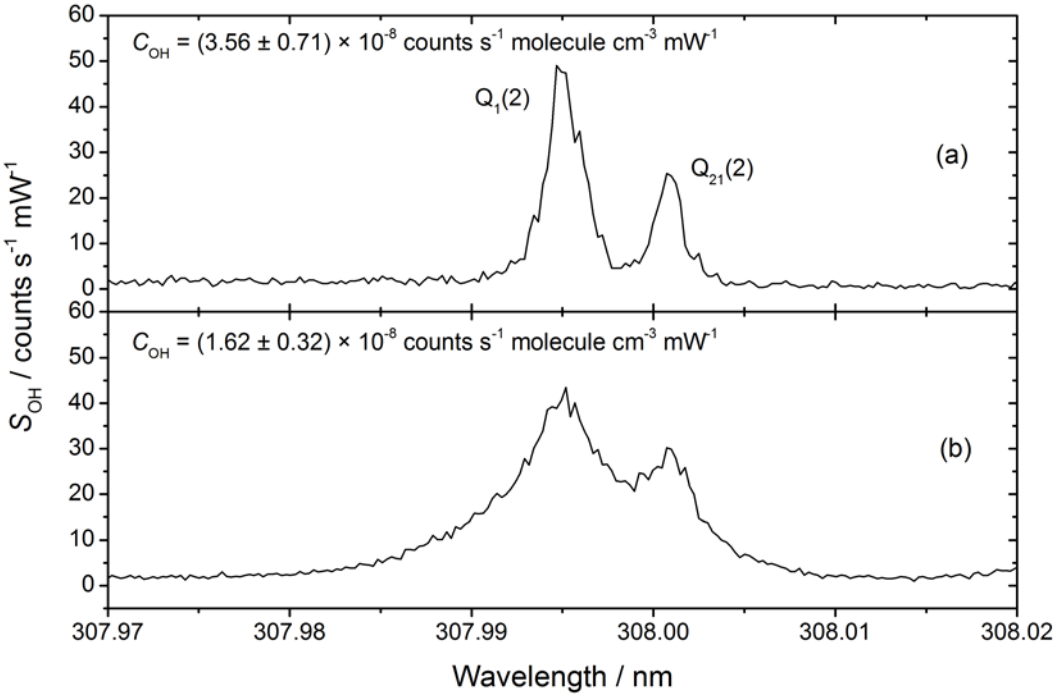

Figure S3. Comparison of the laser excitation spectra for the $Q_1(2)$ and $Q_{21}(2)$ rotational transitions of the OH $A^2\Sigma^+$ (v'=0) ← $X^2\Pi_i$ (v''=0) transition near 308 nm measured using the LITRON pumped dye laser (200 Hz PRF) at 5.0 ± 0.5 mW (a) and 24.0 ± 0.5 mW (b) laser power respectively. The spectrum was recorded at a 0.004 nm grating resolution with 1 second averaging in the OH detection cell maintained at 3.81 mbar (1.0 mm diameter pinhole). Calibration factors, C_{OH}, are quoted to demonstrate the reduction in sensitivity to OH at higher laser powers due to power broadening of the OH LIF line.

Photolysis of a species that could create an excited state OH(v'=0,1) radical upon dissociation could explain the phenomenon. However, as high purity air was used and no species other that

H_2O vapour were introduced into the airflow of the calibration source, this seems unlikely. Laser power broadening of the OH emission is also possible. The increased pulse energy of the 200 Hz PRF laser system (25 μJ $pulse^{-1}$) causes stimulated emission, effectively broadening the measured OH emission bands. No further quantitative analysis was performed, however, and during operation of the instrument laser powers were maintained at (7 ± 1) mW to minimize the effects on HOx radical measurements.

3 Additional calibration plots and data tables.

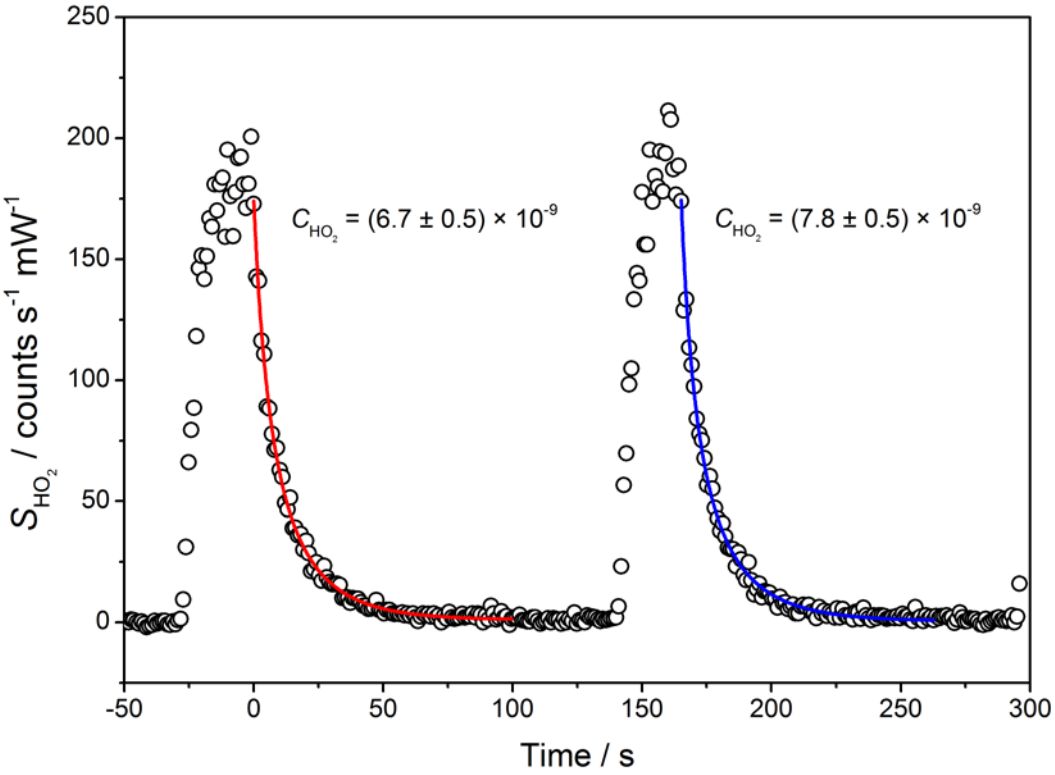

Figure S4. One second averaged HO_2 signal, S_{HO_2}, observed in the HCHO photolysis based alternative HO_2 calibration method at 1.85 mbar internal cell pressure (350 mbar chamber pressure) using the 200 Hz PRF laser system. The S_{HO2} trace demonstrates the mulitple sequential C_{HO_2} factors that can be determined from one experiment. Upon illumination, photoylsis of HCHO led to a sharp increase in S_{HO_2} and t = 0 s denotes the start of the first HO_2 decay analysed when photolysis was stopped. Laser power = 7.5 ± 0.3 mW and $k_{HO_2+HO_2}$ = 2.00 × 10^{-12} cm^3 molecule^{-1} s^{-1} for the multiple non-linear fitting routine (see main text, section 4.2). C_{HO_2} units = counts cm^3 molecule^{-1} s^{-1} mW^{-1}.

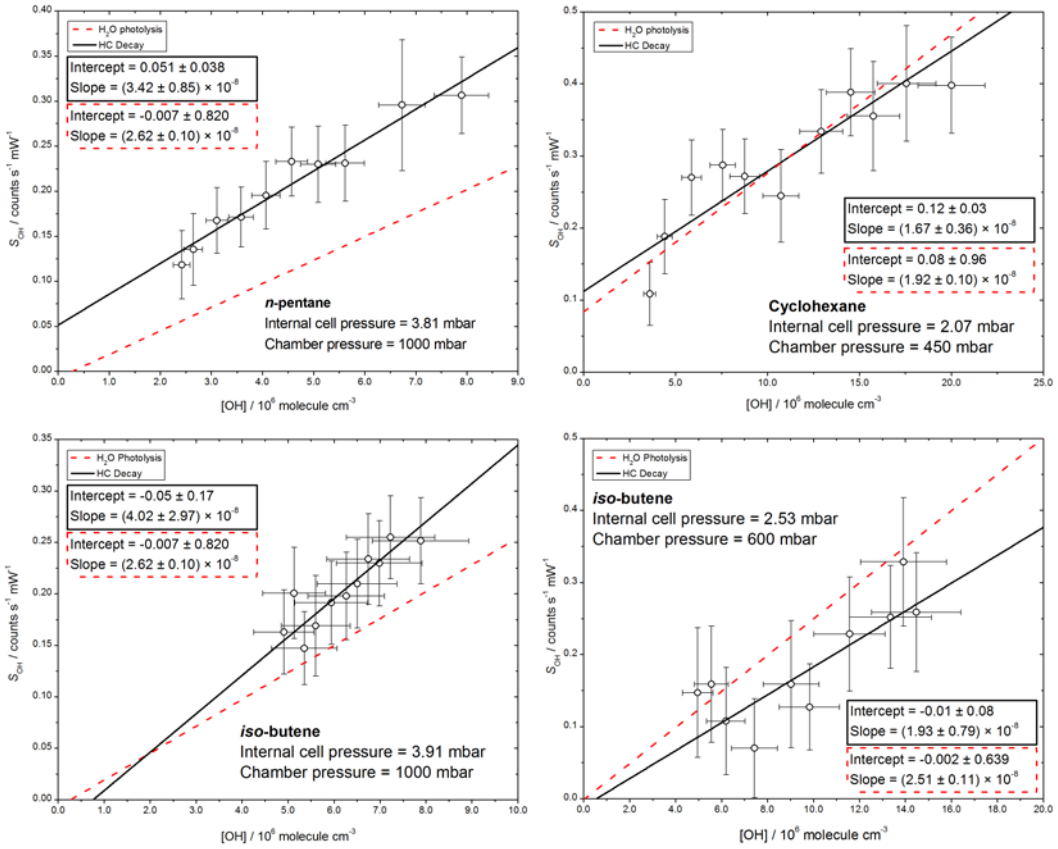

Figure S5. Comparison of four OH calibration plots determined using the newly developed hydrocarbon decay (HC) method for the HIRAC FAGE instrument. Examples are shown for different calibration pressures using different hydrocarbons, compared to the closest pressure calibration factor, C_{OH}, determined using the H_2O photoylsis method. Calibrations were completed at similar laser powers (6 - 8 mW) using the 200 Hz PRF laser system at 60 s averaging. Units: Intercept = counts s^{-1} mW^{-1}, slope = counts cm^3 $molecule^{-1}$ s^{-1} mW^{-1}. Error bars are representative of the precision of the measurements and quoted uncertainties are to ±2σ.

Hydrocarbon	Cell *P* (mbar)	Chamber *P* (mbar)	C_{OH} ($\times 10^{-8}$)	Uncertainty ($\times 10^{-8}$)
n-pentane	3.92	1000	3.42	1.09
iso-butene	3.91	1000	3.08	0.86
	3.91	1000	4.02	2.97
	3.53	880	3.22	1.76
	3.03	750	2.28	0.63
	2.53	600	1.93	0.93
	2.41	550	3.05	1.24
	2.04	450	2.03	1.52
Cyclohexane	3.85	1000	1.93	0.59
	3.83	1000	2.13	0.52
	3.08	750	1.34	0.33
	2.43	550	1.49	0.46
	2.41	550	1.55	0.51
	2.07	450	1.67	0.51

Table S1. Tabulated data from the HC decay alternative OH calibration experiments. Uncertainties quoted to ±2σ and propogated as described in the main text (section 5.4.2). Units for C_{OH} and Uncertianty = counts cm^3 $molecule^{-1}$ s^{-1} mW^{-1}.

Cell *P* (mbar)	Chamber *P* (mbar)	C_{HO_2} ($\times 10^{-8}$)	Avg. C_{HO_2} ($\times 10^{-8}$)	Uncertainty ($\times 10^{-8}$) ±2σ
3.91	1000	1.54 1.37 1.72 1.47 1.63	1.55	0.52
3.67	880	1.71 1.96 1.65 2.51 2.26	2.02	0.74
2.52	550	1.57 1.27 1.35 1.32	1.38	0.52
2.05	410	0.68 1.78 0.98 0.78	1.06	0.44
1.85	350	1.12 0.67 0.78	0.86	0.40

Table S2. Tabulated data from the HCHO photolysis based alternative HO_2 calibration experiments for the HIRAC FAGE instrument. Uncertainties quoted to ±2σ and propogated as described in the main text (section 5.4.3). Units for C_{HO_2}, Avg. C_{HO_2} and Uncertianty = counts cm^3 $molecule^{-1}$ s^{-1} mW^{-1}.

		Mixing Fans On			Mixing Fans Off		
Cell *P* (mbar)	Chamber *P* (mbar)	C_{HO_2} ($\times 10^{-7}$)	Avg. C_{HO_2} ($\times 10^{-7}$)	Uncertainty ($\times 10^{-7}$) $\pm 2\sigma$	C_{HO_2} ($\times 10^{-7}$)	Avg. C_{HO_2} ($\times 10^{-7}$)	Uncertainty ($\times 10^{-7}$) $\pm 2\sigma$
2.48	1000	1.70 0.72 1.06 0.90 1.13	1.10	0.19	0.99 0.95 1.57 0.92	1.11	0.21
2.10	850	0.72 1.21 0.78	0.90	0.20	0.76 0.68	0.72	0.19
1.84	730	0.82 0.49 0.69	0.67	0.15	0.61 0.79	0.70	0.19
-	-	-	-	-	0.54 0.48	0.51	0.13
1.42	500	0.65 0.51 1.05	0.73	0.28	0.47 0.76	0.62	0.21

Table S3. Tabulated data from the HCHO photolysis based alternative HO_2 calibration experiments for the aircraft FAGE instrument. Uncertainties quoted to $\pm 2\sigma$ and propogated as described in the main text (section 5.4.3). Units for C_{HO_2}, Avg. C_{HO_2} and Uncertianty = counts cm^3 $molecule^{-1}$ s^{-1} mW^{-1}.